

Exploiting Inter-Sample Affinity for Knowability-Aware Universal Domain Adaptation

Yifan Wang^{1*}, Lin Zhang^{1*}, Ran Song¹, Lin Ma², and Wei Zhang¹

¹ Vsislab, Shandong University
17923 Jingshi Rd., Lixia Dist., Jinan, Shandong, China
info@vsislab.com

² MeiTuan

Abstract. Universal domain adaptation (UDA) aims to transfer the knowledge of common classes from source domain to target domain without any prior knowledge on the label set, which requires to distinguish the unknown samples from the known ones in the target domain. Recent methods preferred to increase the inter-sample affinity within a known class, while they ignored the inter-sample affinity between the unknown samples and the known ones. This paper reveals that exploiting such inter-sample affinity can significantly improve the performance of UDA and proposes a knowability-aware UDA framework based on it. First, we estimate the knowability of each target sample by searching its neighboring samples in the source domain. Then, we propose an auto-thresholding scheme applied to the estimated knowability to determine whether a target sample is unknown or known. Next, in addition to increasing the inter-sample affinity within each known class like previous methods, we design new losses based on the estimated knowability to reduce the inter-sample affinity between the unknown target samples and the known ones. Finally, experiments on four public datasets demonstrate that our method significantly outperforms existing state-of-the-art methods.

Keywords: Universal Domain Adaptation, Open Class Detection

1 Introduction

Unsupervised domain adaptation (DA) [8,23,15,9,29] aims to transfer the learned knowledge from the labeled source domain to the unlabeled target domain so that the inter-sample affinities in the latter can be properly measured. The assumption of traditional unsupervised DA, i.e. closed-set DA, is that the source domain shares identical label set with the target domain, which significantly limits its applications in real-world scenarios. Thus, relaxations to this assumption have been investigated. Partial-set DA (PDA) [3,4,28,13] assumes that target domain is not identical to source domain but its subset. On the contrary, Open-set DA (ODA) [16,24,14] assumes that target domain contains

classes *unknown* to the source domain such that the source domain is a subset of the target domain. Open-partial DA (OPDA) [22,12,7] introduces private classes in both domains respectively, where the private classes in the target domain are unknown, and assumes that the common classes shared by the two domains have been identified. Universal DA (UDA) [1,22,12] concerns about unsupervised DA with the most general setting, where no prior knowledge is required on the label set relationship between domains.

A popular method [27,1,7] for UDA is to employ a classifier which produces a confidence of each sample to determine whether it belongs to a particular known class seen in the source domain or the unknown class. In essence, they treated the unknown class and each known class equally. However, compared to the inter-sample affinity in a known object class, that in the unknown class is semantically much larger as the unknown class usually contains samples that semantically belong to different object classes. This means that the inter-sample affinity between two samples in the unknown class could be even lower than that between a sample in the unknown class and a sample in a known object class. As a result, some unknown samples could be incorrectly classified into some known classes.

To solve this problem, some recent approaches aim to increase the inter-sample affinity within a known class to improve the reliability of the classification. For instance, Li *et al.* [12] solved this problem by replacing the classifier-based framework with a clustering-based one which exploited the intrinsic structure of samples and thus increased the inter-sample affinity in each cluster. Saito *et al.* [22] proposed a simple one-vs-all framework for UDA to increase the inter-sample affinity in a known class by making each known class more compact and achieved the state-of-the-art (SOTA) performance. However, we found that the aforementioned methods did not consider reducing the inter-sample affinity between the unknown samples and all known ones, which is also important for avoiding the incorrect classification.

Therefore, we propose to better exploit the inter-sample affinity for UDA. In particular, apart from the inter-sample affinity within a known class, that between an unknown sample and a known one should also be taken into account. To achieve this, we first introduce the concept of *knowability* for each target sample and compute it based on the neighborhood of each target sample. To construct such a neighborhood, we use the k -nearest neighbors (k -NN) algorithm to find a set of source samples as the neighbors of each target sample. Then, a target sample is labeled as *known*, *unknown* or *uncertain* through an automatic thresholding scheme based on its knowability score. Next, we design three losses to impose a restriction to the unknown and known samples. The restriction aims to 1) reduce the inter-sample affinity between the unknown samples and the known ones in the target domain and 2) increase the inter-sample affinity between the known samples in the target domain and some particular samples found by the k -NN algorithm in the source domain where such target and source samples are supposed to belong to the same known class.

In addition, the thresholding based on the knowability score is not straightforward. We also notice that as pointed in [22], existing methods usually require to manually set a threshold to distinguish the unknown samples from the known ones. To address this problem, we further introduce a knowability-aware auto thresholding scheme to automatically adjust the threshold on-the-fly, which avoids setting the threshold manually for each dataset.

The contributions of this paper are thus threefold:

- We propose a novel knowability estimation based on the neighborhood searching cross-domain to pre-classify a target sample as the known or unknown sample based on the consistency of its neighbors in source domain.
- We introduce three losses of target domain based on the results of the knowability estimation to reduce the inter-sample affinity between the unknown classes and the known classes while increase that in a known object class in the target domain.
- We propose an automatic scheme to produce a threshold for the knowability estimation on-the-fly which adapts to the change of the distribution of the knowability score of all target samples at different datasets.

2 Related Work

We briefly review recent unsupervised DA methods in this section. According to the assumption made about the relationship between the label sets of different domains, we group these methods into three categories, namely PDA, ODA and UDA.

2.1 Partial-set Domain Adaptation

PDA requires that the source label set is larger than and contains the target label set. Many methods for PDA have been developed [2,3,28,4,13]. For example, Cao *et al.* [2] presented the selective adversarial network (SAN), which simultaneously circumvented negative transfer and promoted positive transfer to align the distributions of samples in a fine-grained manner. Zhang *et al.* [28] proposed to identify common samples associated with domain similarities from the domain discriminator, and conducted a weighting operation based on such similarities for adversarial training. Cao *et al.* [4] proposed a progressive weighting scheme to estimate the transferability of source samples. Liang *et al.* [13] introduced balanced adversarial alignment and adaptive uncertainty suppression to avoid negative transfer and uncertainty propagation.

2.2 Open-set Domain Adaptation

ODA, first introduced by Busto *et al.* [16], assumes that there are private and common classes in both source and target domains, and common class labels are known as prior knowledge. They introduced the Assign-and-Transform-Iteratively (ATI) algorithm to address this challenging problem. Recently, one of

the most popular strategies [14,6] for ODA is to draw the knowledge from the domain discriminator to identify common samples across domains. Saito *et al.* [24] proposed an adversarial learning framework to obtain a boundary between source and target samples whereas the feature generator was trained to make the target samples far from the boundary. Bucci *et al.* [1] employed self-supervised learning technique to achieve the known/unknown separation and domain alignment.

2.3 Universal Domain Adaptation

UDA, first introduced by You *et al.* [27] is subject to the most general setting of unsupervised DA, which involves no prior knowledge about the difference on object classes between the two domains. You *et al.* also presented an universal adaptation network (UAN) to evaluate the transferability of samples based on uncertainty and domain similarity for solving the UDA problem. However, the uncertainty and domain similarity measurements are sometimes not robust and sufficiently discriminative. Thus, Fu *et al.* [7] proposed another transferability measure, known as Calibrated Multiple Uncertainties (CMU), estimated by a mixture of uncertainties which accurately quantified the inclination of a target sample to the common classes. Li *et al.* [12] introduced Domain Consensus Clustering (DCC) to exploit the domain consensus knowledge for discovering discriminative clusters on the samples, which differed the unknown classes from the common ones. The latest work OVANet [22], proposed by Saito *et al.*, trained a one-vs-all classifier for each class using labeled source samples and adapted the open-set classifier to the target domain.

3 Method

In this section, we elaborate the major components of the proposed knowability-aware UDA framework which sufficiently exploits the inter-sample affinity as stated in the introduction.

Notation Assume that we have the labeled set of source samples $\mathcal{X}^s = \{x_i^s\}_{i=1}^{n^s}$ defined with the known space of the source label set \mathcal{Y}^s and the unlabeled set of target samples $\mathcal{X}^t = \{x_i^t\}_{i=1}^{n^t}$ where n^s and n^t indicate the numbers of the source and the target samples, respectively. Since the label spaces of the two domains are not aligned, we have the space of the target label set $\mathcal{Y}^t = \mathcal{Y}^{com} \cup \mathcal{Y}^{unk}$ with $\mathcal{Y}^{com} \subseteq \mathcal{Y}^s$. \mathcal{Y}^{com} and \mathcal{Y}^{unk} denote the spaces for the common label set and the unknown label set respectively where $\mathcal{Y}^{unk} \cap \mathcal{Y}^s = \emptyset$. With the training samples from both domains, the goal of UDA is to learn an optimal classifier $C^t : \mathcal{X}^t \rightarrow \mathcal{Y}^t$ which categorizes a target sample into either \mathcal{Y}^{unk} or an object class belonging to \mathcal{Y}^{com} .

3.1 Overall Workflow

As shown in Fig. 1, we first extract a feature f_i from a sample x_i by the feature extractor $\mathcal{F}(\cdot|\phi)$ where \cdot represents an input sample and ϕ denotes the set

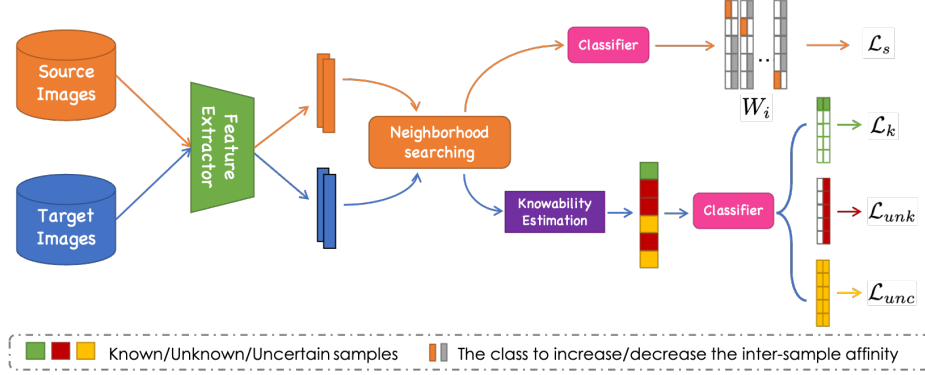


Fig. 1. The overall workflow of the proposed knowability-aware UDA framework which heavily exploits the inter-sample affinity.

of trainable parameters of the feature extractor. Then, we search neighbors from the source domain for each sample in both domains. Next, we establish an inter-sample affinity weight matrix W_i for each sample in the source domain based on its neighbors. W_i is then incorporated into a loss function \mathcal{L}_s . Through training, the proposed method increases the inter-sample affinity within each class in the source domain while decreasing that between the samples of different classes in the source domain. For the target samples, we categorize them into *known*, *unknown* and *uncertain* classes based on their knowability scores produced by the knowability estimation scheme. We then design three losses, expressed as \mathcal{L}_k , \mathcal{L}_{unk} , and \mathcal{L}_{unc} for the three classes of samples, which set desired restrictions on them respectively by exploiting the inter-sample affinities. Finally, we employ one classifier $\mathcal{C}(\cdot|\theta)$ defined in Eq. (1) to classify all samples subject to the four losses:

$$\mathcal{C}(\cdot|\theta) : \mathbf{x} \rightarrow \begin{bmatrix} \mathcal{C}_1^{(1)}(\cdot|\theta), \mathcal{C}_1^{(2)}(\cdot|\theta), \dots, \mathcal{C}_1^{(Y)}(\cdot|\theta) \\ \mathcal{C}_2^{(1)}(\cdot|\theta), \mathcal{C}_2^{(2)}(\cdot|\theta), \dots, \mathcal{C}_2^{(Y)}(\cdot|\theta) \end{bmatrix}^T \quad (1)$$

where θ denotes the set of parameters of the classifier implemented through a fully-connected layer. $\mathcal{C}_1^{(j)}(\cdot|\theta) + \mathcal{C}_2^{(j)}(\cdot|\theta) = 1$, and $\mathcal{C}_1^{(j)}$ and $\mathcal{C}_2^{(j)}$ represent the probabilities that a sample x_i^t is accepted or rejected as a member of an object class with index y in \mathcal{Y}^s containing Y object classes, respectively. In the testing stage, for a target sample x_i^t , we define the reject score of x_i^t as the minimum value of reject probabilities. If $\min_{j \in [1 \dots Y]} (\mathcal{C}_2^{(j)}(x_i^t|\theta)) > 0.5$, we regard x_i^t as an unknown sample and otherwise a known sample while the label $y_i = \operatorname{argmax}_{j \in [1 \dots Y]} (\mathcal{C}_1^{(j)}(x_i^t|\theta))$.

It is noteworthy that a threshold is needed to determine whether a sample is known or unknown based on its knowability score. However, it is difficult to find a fixed threshold which suits well with different datasets. To avoid setting such a threshold manually for each dataset, we also propose a knowability-aware auto-

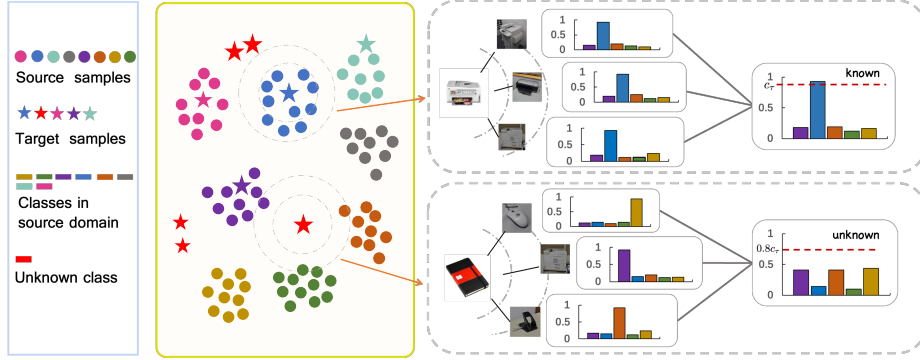


Fig. 2. Overview of the knowability estimation. We find the k -nearest neighbors from the source domain for each target sample. The knowability score of each target sample is computed as the maximum value of the average accepting probabilities of all the neighbors for each target sample.

thresholding scheme to dynamically produce the threshold optimal to varying datasets.

3.2 Knowability-Aware Target-Domain Losses Based on Inter-Sample Affinity

To reduce the inter-sample affinity between the unknown samples and the known ones and increase that within a known class, we first propose an unified knowability estimation scheme to pre-classify the unknown samples and some reliably known ones in the target domain by retrieving the neighbors of each target sample from the source domain.

Intuitively, the neighbors in the source domain of an unknown sample in the target domain are likely to have inconsistent classes labels since the unknown sample does not belong to any source class. In contrast, a known target sample should be close to a group of source samples belonging to the same class and thus its neighbors are more likely to have consistent class labels. Specially, for each sample x_i^t in the target domain, we retrieve its k -nearest neighbors from the samples in the source domain based on the L2-distance. And then we leverage the accepting probabilities of each neighbor produced by the classifier to compute the knowability score c_i :

$$c_i = \max_{j \in [1 \dots Y]} \left(\frac{1}{|\mathcal{N}_i|} \sum_{k \in \mathcal{N}_i} \mathcal{C}_1^{(j)}(m_k | \theta) \right) \quad (2)$$

where \mathcal{N}_i denotes the set of indexes of the k -nearest neighbors in the source domain of the target sample x_i^t . The higher the knowability score, the more likely the sample belongs to a known class. And a lower knowability score represents that the target sample belongs to the unknown class.

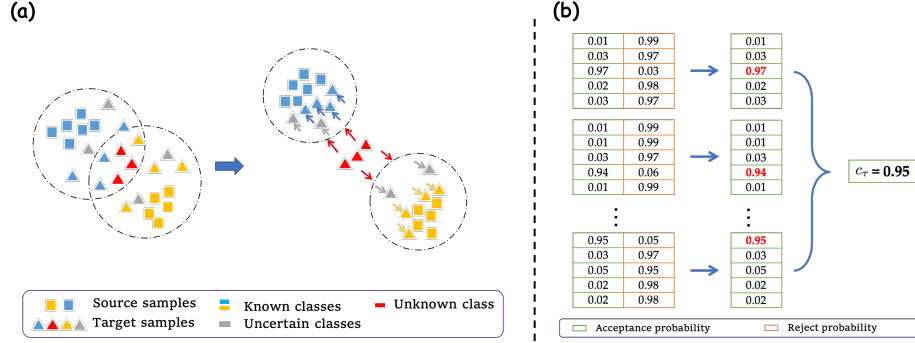


Fig. 3. (a) The effect of the target-domain losses. The blue and yellow arrows represent the effect of \mathcal{L}_k , the red arrows represent the effect of \mathcal{L}_{unk} , and the gray arrows represent the effect of \mathcal{L}_{unc} . (b) The knowability-aware auto-thresholding. In every step, we compute the average of the maximum accepting probabilities of the source samples in the mini-batch as c_τ .

Formally, if $c_i < 0.8c_\tau$, we regard x_i^t as an unknown sample. Note that the threshold c_τ is produced automatically as detailed in Sec. 3.3 and 0.8 is chosen empirically. Then, if $c_i > c_\tau$, x_i^t is recognized as a known sample. If $0.8c_\tau < c_i < c_\tau$, x_i^t is regarded as an uncertain sample.

For an unknown sample, we hope to push the samples of all known classes away from it as shown in Fig. 3(a) for reducing the inter-sample affinity between the unknown samples and the known ones. Thus we design the target-domain loss for the unknown samples, \mathcal{L}_{unk} , which minimizes the entropy of the reject probabilities for all classes to maximum all reject probabilities:

$$\mathcal{L}_{unk}(x_i^t) = -\frac{1}{Y} \sum_{j=1}^Y \mathcal{C}_2^{(j)}(x_i^t|\theta) \log(\mathcal{C}_2^{(j)}(x_i^t|\theta)) \quad (3)$$

For the known samples in the target domain, we define the pseudo label of x_i^t as:

$$\hat{y}_i^t = \operatorname{argmax}_{j \in [1 \dots Y]} (\sum_{k \in \mathcal{N}_i} \mathcal{C}_1^{(j)}(x_k^s|\theta)) \quad (4)$$

where $\operatorname{argmax}(\cdot)$ denotes the index of the biggest value in a vector. Since the discrepancies exist between source samples and target samples belonging to the same object class due to the domain gap, the inter-sample affinity between them cannot be as high as that between the source samples belonging to the same object class. Thus, as shown in Fig. 3(a), to increase the inter-sample affinity within a known class in the target domain, we increase the inter-sample affinity between the known samples in the target domain and the corresponding samples with the pseudo label \hat{y}_i^t in the source domain. This is achieved by designing the target-domain loss \mathcal{L}_k which minimizes the entropy of the accepting probability of class \hat{y}_i^t :

$$\mathcal{L}_k(x_i^t) = -\mathcal{C}_1^{(\hat{y}_i^t)}(x_i^t|\theta) \log(\mathcal{C}_1^{(\hat{y}_i^t)}(x_i^t|\theta)) \quad (5)$$

For the uncertain samples, we do not push them to a certain class but leverage a loss \mathcal{L}_{unc} to minimize the average entropy of all the classifiers to keep the inter-sample affinities low in every known classes:

$$\mathcal{L}_{unc}(x_i^t) = -\frac{1}{2Y} \sum_{k=1,2} \sum_{j=1}^Y \mathcal{C}_k^{(j)}(x_i^t|\theta) \log \left(\mathcal{C}_k^{(j)}(x_i^t|\theta) \right) \quad (6)$$

3.3 Knowability-Aware Auto-Thresholding

Distinguishing the unknown samples from the known ones in the target domain is obviously affected by the choice of a threshold c_τ . However, varying sizes and categories of different datasets lead to the change of the optimal threshold. In order to avoid setting the threshold manually for each dataset, we introduce a knowability-aware auto-thresholding scheme.

Specifically, as shown in Fig. 3(b), for a source sample x_i^s , we compute the maximum value of the accepting probabilities $\mathcal{C}_1(x_i^s|\theta)$ as its knowability score. Then, the threshold c_τ is calculated as the average knowability score of the source samples in the mini-batch:

$$c_\tau = \frac{1}{|\mathcal{B}|} \sum_{i=1}^{|\mathcal{B}|} \max_{j \in [1..Y]} \left(\mathcal{C}_1^{(j)}(x_i^s|\theta) \right) \quad (7)$$

where $|\mathcal{B}|$ represents the size of the mini-batch. This scheme avoids setting different thresholds for different datasets manually.

3.4 Source-Domain Loss Based on Inter-Sample Affinity

For a sample x_i^s in the source domain with label y_i^s , to deliver a reliable classification, we should increase the inter-sample affinity within class y_i^s and reduce that between class y_i^s and other classes in the source domain. Thus, we propose the inter-sample affinity weight matrix $W_i = [v_1, v_2]^T$ for x_i^s where $v_1, v_2 \in \mathbb{R}^Y$ represent the weights associated with the classes which require to increase or decrease the inter-sample affinity, respectively. In detail, $v_1 = (\mathbb{1}(j = y_i^s))_{j=1}^Y$ is the one-hot vector of class y_i^s . And v_2 is computed based on the inter-sample affinities between x_i^s and the samples from other source classes by retrieving the k -nearest neighbors of x_i^s from the samples with the labels different from y_i^s in the source domain, expressed as:

$$v_2 = \left(\text{normalize} \left(\frac{|N_i^{(j)}|}{|\mathcal{N}_i^s|} * \frac{\mathcal{C}_1^{(j)}(x_i^s|\theta)}{\sum_{k \neq y_i^s} \mathcal{C}_1^{(k)}(x_i^s|\theta)^2} \right) \right)_{j=1}^Y \quad (8)$$

where the *normalize* denotes the L1-normalization. $|N_i^{(j)}|$ and $|\mathcal{N}_i^s|$ represent the number of the neighbors belonging to the label y_j^s and the total number of the

retrieving neighbors of x_i^s respectively and note that $v_2^{y_i^s}$ is set to 0. According to in Eq. (8), the larger values in v_2 means that the samples in class i are closer to x_i^s . Then, we compute the source-domain loss $\mathcal{L}_s(x_i^s)$ based on the weighted inter-sample affinity:

$$\mathcal{L}_s(x_i^s) = -\log \langle W_i, \mathcal{C}(x_i^s | \theta) \rangle \quad (9)$$

where $\langle \cdot, \cdot \rangle$ is the dot product operator.

3.5 Overall Loss for Both Domains

Overall, we train the classifier $\mathcal{C}(\cdot | \theta)$ and the feature extractor $\mathcal{F}(\cdot | \phi)$ with four losses and a hyper-parameter λ . The overall loss is expressed as:

$$\mathcal{L}_{all} = \mathcal{L}_s + \lambda(\mathcal{L}_{unk} + \mathcal{L}_k + \mathcal{L}_{unc}) \quad (10)$$

It is worth mentioning that differing from many existing UDA methods [12, 1, 7, 21], there is only one hyper-parameter in our method.

4 Experimental Results

In this section, we first introduce our experimental setups, including datasets, evaluation protocols and training details. Then, we compare our method with the SOTA UDA methods. We also conduct extensive ablation studies to demonstrate the effectiveness of each component of the proposed method. All experiments were implemented on one RTX2080Ti 11GB GPU with PyTorch 1.7.1 [17]. More results can be found in the supplementary material.

4.1 Experimental setups

Datasets and evaluation protocols. We conduct experiments on four datasets. Office-31 [20] consists of 4,652 images from three domains: DSLR (D), Amazon (A), and Webcam (W). OfficeHome [18] is a more challenging dataset, which consists of 15,500 images from 65 categories. It is made up of 4 domains: Artistic images (Ar), Clip-Art images (Cl), Product images (Pr), and Real-World images (Rw). VisDA [19] is a large-scale dataset, where the source domain contains 15,000 synthetic images and the target domain consists of 5,000 images from the real world. DomainNet [26] is a larger DA dataset containing around 0.6 million images.

In this paper, we use the **H-score** in line with recent UDA methods [7, 12, 22]. H-score, proposed by Fu *et al.* [7], is the harmonic mean of the accuracy on the common classes a_{com} and the accuracy on the unknown class a_{unk} :

$$h = \frac{2a_{com} \cdot a_{unk}}{a_{com} + a_{unk}}. \quad (11)$$

Table 1. Results on Office-31 with UDA setting (H-score)

Method	Office-31 (10/10/11)						Avg
	A2D	A2W	D2A	D2W	W2D	W2A	
UAN [27]	59.7	58.6	60.1	70.6	71.4	60.3	63.5
CMU [7]	68.1	67.3	71.4	79.3	80.4	72.2	73.1
DANCE [21]	78.6	71.5	79.9	91.4	87.9	72.2	80.3
DCC [12]	88.5	78.5	70.2	79.3	88.6	75.9	80.2
ROS [1]	71.4	71.3	81.0	94.6	95.3	79.2	82.1
USFDA [11]	85.5	79.8	83.2	90.6	88.7	81.2	84.8
OVANet [22]	85.8	79.4	80.1	95.4	94.3	84.0	86.5
Ours	88.9	83.0	81.1	94.5	98.3	85.2	88.5

Table 2. H-score of Universal DA using OfficeHome

Method	OfficeHome (10/5/50)												Avg
	A2C	A2P	A2R	C2A	C2P	C2R	P2A	P2C	P2R	R2A	R2C	R2P	
OSBP[24]	39.6	45.1	46.2	45.7	45.2	46.8	45.3	40.5	45.8	45.1	41.6	46.9	44.5
UAN[27]	51.6	51.7	54.3	61.7	57.6	61.9	50.4	47.6	61.5	62.9	52.6	65.2	56.6
CMU[7]	56.0	56.9	59.1	66.9	64.2	67.8	54.7	51.0	66.3	68.2	57.8	69.7	61.6
OVANet[22]	62.8	75.6	78.6	70.7	68.8	75.0	71.3	58.6	80.5	76.1	64.1	78.9	71.8
Ours	63.9	79.0	83.5	70.4	72.4	77.6	71.7	61.3	83.6	78.8	64.3	83.0	73.8

Training details. We employ the ResNet-50 [10] backbone pretrained on ImageNet[5] and optimize the model using Nesterov momentum SGD with momentum of 0.9 and weight decay of 5×10^{-4} . The batch size is set to 36 through all datasets. The initial learning rate is set as 0.01 for the new layers and 0.001 for the backbone layers. The learning rate is decayed with the inverse learning rate decay scheduling. The number of neighbors retrieved is set to be dependent on the sizes of the dataset. For Office-31 (4,652 images in 31 categories) and OfficeHome (15,500 images in 65 categories), the number of retrieved neighbors $|\mathcal{N}_i|$ is set to 10. For VisDA (20,000 images in total) and DomianNet (0.6 million images), we set $|\mathcal{N}_i|$ to 100, respectively. We set λ to 0.1 which is constant through all the datasets.

4.2 Comparison with the SOTA Methods

Baselines. We aim to show that pre-classifying some unknown/known samples is effective for UDA by comparing our method with the current SOTA methods, such as UAN [27] and CMU [7], which employed a classifier to produce the confidence of each sample to determine whether it belongs to the unknown class or not. Also, we compare our method with OVANet [22] to show that it is important to reduce the inter-sample affinity between the unknown samples and the known ones.

Results in main datasets. Tables 1 and 2 list the results on Office-31 and OfficeHome, respectively. On Office-31, our method outperforms the SOTA methods by 2.0% in terms of the H-score on average. For the more challenging dataset

Table 3. Results on DomainNet and VisDA with UDA setting (H-score)

Method	DomainNet (150/50/145)						Avg	VisDA (6/3/3)
	P2R	R2P	P2S	S2P	R2S	S2R		
DANCE [21]	21.0	47.3	37.0	27.7	46.7	21.0	33.5	4.4
UAN [27]	41.9	43.6	39.1	38.9	38.7	43.7	41.0	30.5
CMU [7]	50.8	52.2	45.1	44.8	45.6	51.0	48.3	34.6
DCC [12]	56.9	50.3	43.7	44.9	43.3	56.2	49.2	43.0
OVANet [22]	56.0	51.7	47.1	47.4	44.9	57.2	50.7	53.1
Ours	59.1	52.4	47.5	48.1	45.1	58.6	51.8	54.7

OfficeHome which contains much more private classes than common classes, our method also made a significant improvement of 2.0% in terms of the H-score. Our method consistently performs better than other methods. VisDA is a much larger dataset than Office-31 and OfficeHome which contains about 10000 images in each domain. DomainNet is the largest dataset for UDA. our method achieves the SOTA performance on both datasets as shown in Table 3.

Summary. According to the results of quantitative comparisons, our method achieves the SOTA performance in every dataset and most sub-tasks, which demonstrates the main idea of our method that reduces the inter-sample affinity between the unknown samples and the known ones.

4.3 Ablation Studies

Effect of pre-classifying. To show the effect of pre-classifying, first, we plot the distributions of the reject scores of all sample in the target domain at the final epoch in Fig. 4(a). Then, we compare the plot to that without the pre-classifying, which means that all samples are regarded as uncertain samples in Fig. 4(b). We can observe that the full version of our method better distinguish the known samples from the unknown ones. Furthermore, in Fig. 4(c), we show the corresponding plot produced by OVANet [22] for comparison. Noticeably, our method performs better than OVANet [22] in terms of distinguishing the known samples from the unknown ones.

Then, we use t-SNE to visualize features extracted by $\mathcal{F}(\cdot|\phi)$ for the model trained only with the source samples, OVANet and the proposed method on Office-31(A2D). As shown in Fig. 5, before the adaptation to the target domain (left), there exist significant misalignment. After the adaptation with the training via OVANet (middle) and our method (right), the features become more discriminative. We observe better domain alignment as well as target category separation produced by our method. Note that although OVANet does succeed in aligning the source and target domains and can detect the unknown class, but it does not necessarily produce discriminative features for each known class. Moreover, compared to the model trained only with the source samples, the visualization of our method shows that the inter-sample affinity in each known class increases while that between different classes decreases. More visualizations (i.e.

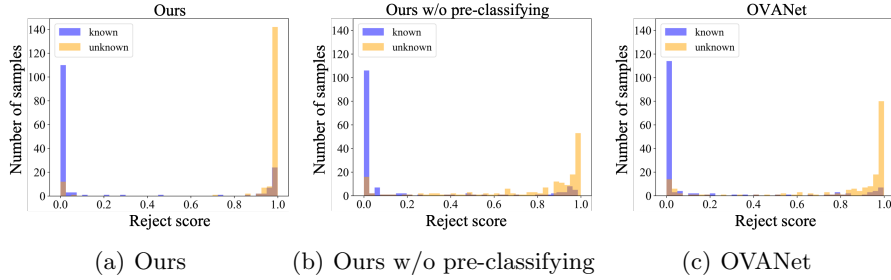


Fig. 4. Effect of knowability-aware scheme. The three plots of histograms show the reject scores at the last epoch produced by the full version of our method, our method without pre-classifying and OVANet [22] in Office-31(A2D) respectively. Each brown area indicates that there is an overlap between the blue and the yellow colors.

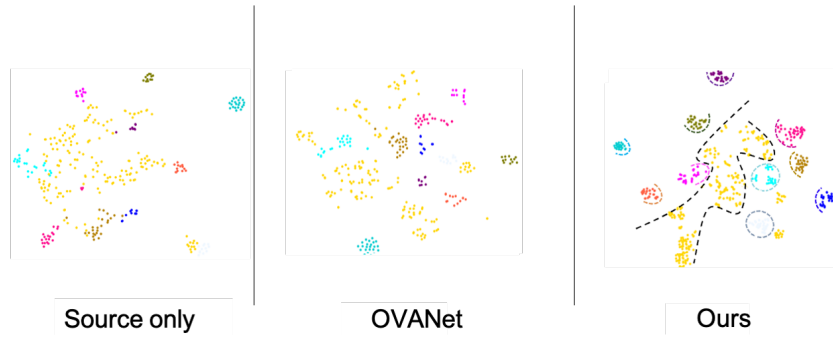


Fig. 5. The t-SNE visualizing cooperation. Different colors represent different classes. Yellow points represent the unknown samples while the points in other colors represent the known samples of different classes. The black dash lines represent the boundaries between the unknown samples and the known ones while the dash lines in other colors represent the boundaries of the corresponding known classes.

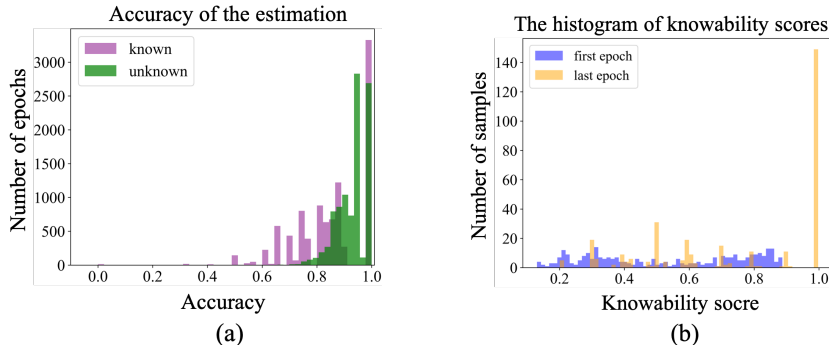
histograms and t-SNE) of the results in different sub-tasks can be found in the supplementary material.

Accuracy of the knowability estimation. We conducted experiments on Office-31(A2D) where we recorded the accuracy of the knowability estimation of the unknown and known samples at different training epochs. As plotted in Fig. 6(a), the knowability is consistently estimated with high accuracy which far surpasses 80% on average for both known and unknown samples. Thus, through the proposed knowability estimation scheme, our approach finds the unknown and the known samples in the target domain reliably. More plots for other sub-tasks can be found in the supplementary material.

Effect of the proposed losses. We conduct the experiment to show the change of the distribution of knowability scores, which demonstrates that training with

Table 4. Results of different ablated versions of our method on Office-31.

Method	Office-31 (10/10/11)						Avg
	A2D	A2W	D2A	D2W	W2D	W2A	
w/o \mathcal{L}_s	29.2	33.4	31.3	52.5	44.2	27.9	36.4
w/o \mathcal{L}_{unk}	81.0	77.5	78.2	95.0	91.0	72.9	82.6
w/o \mathcal{L}_{unc}	86.9	76.6	84.4	91.4	93.3	85.6	86.3
w/o \mathcal{L}_k	86.2	80.6	79.5	93.9	97.5	81.8	86.5
Ours	89.5	84.9	89.7	93.7	85.8	88.5	88.7


Fig. 6. (a) The accuracy of the knowability estimation on Office-31(A2D). (b) The distributions of knowability scores of the first and the last epochs on Office-31(A2D).

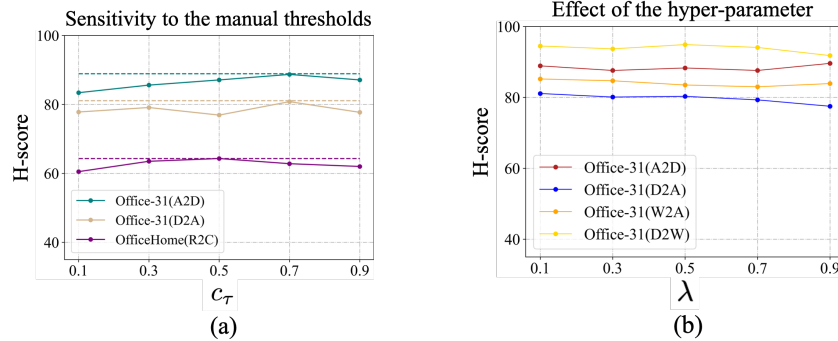
the proposed losses can increase the inter-sample affinity among the known samples belonging to the same object class and reduce that between the unknown samples and the known ones. Fig. 6(b) plots the histogram of the distributions of knowability scores corresponding to the first and the last epochs. It can be seen that in the last epoch, the distribution is more discriminative than that in the first epoch. This means that through the training, the neighbors of each known sample become more reliable and increase its knowability. More histograms of different sub-tasks can be found in the supplementary material.

We also provide an ablation study to investigate the effect of each loss in our UDA framework. As shown in Table 4, each loss is effective. In particular, among the three target-domain losses, \mathcal{L}_{unk} has the largest impact on the final performance, which demonstrate that it is highly important to reduce the inter-sample affinity between the unknown samples and the known ones.

Performance on VGGNet [25]. Table 5 shows the quantitative comparison with the ODA setting on Office-31 using VGGNet[25] instead of ResNet50 as the backbone for feature extraction. According to the results, we demonstrate that our method is also effective with another backbone without changing any hyper-parameters.

Table 5. Results on Office-31 using the VGGNet [25] backbone with the ODA setting.

Method	Office-31 (10/10/11)						Avg
	A2D	A2W	D2A	D2W	W2D	W2A	
OSBP [24]	81.0	77.5	78.2	95.0	91.0	72.9	82.6
ROS [1]	79.0	81.0	78.1	94.4	99.7	74.1	84.4
OVANet [22]	89.5	84.9	89.7	93.7	85.8	88.5	88.7
Ours	89.4	85.6	92.4	94.5	90.5	92.2	90.8

**Fig. 7.** (a) Results of different human-picked thresholds in terms of H-score while the dash lines represent the results of the proposed auto-thresholding scheme. (b) Sensitivity to λ in terms of H-score.

Effect of knowability-aware auto-thresholding. To show the effect of the knowability-aware auto-thresholding scheme, we compare it with the human-picked thresholds on Office-31(A2D, D2A) and OfficeHome(R2C). From Fig. 7(a), we can observe that it is difficult to choose a consistently optimal threshold for all datasets and sub-tasks as the model is sensitive to the thresholds.

Sensitivity of the hyper-parameter λ . There are only one hyper-parameter λ in our model. To show the sensitivity of λ in the total loss, we conducted experiments on Office-31 with the UDA setting. Fig. 7(b) shows that our method has a highly stable performance over different values of λ .

5 Conclusions

In this paper, we propose a new framework to explore the inter-sample affinity for UDA. Its core idea is to reduce the inter-sample affinity between the unknown samples and the known ones while increasing that within the known samples by estimating the knowability of each sample. Also, our method automatically adapts to the varying distributions of the knowability scores of the target samples in different datasets. As demonstrated by extensive experiments, our method sets the new SOTA performance in various sub-tasks on four public datasets.

A limitation of our method is that it does not sufficiently utilize the inter-sample relationship within the set of unknown samples. Thus in the future work,

we plan to extend our method to leverage this relationship for further boosting the performance with the UDA setting.

References

1. Silvia Bucci, Mohammad Reza Loghmani, and Tatiana Tommasi. On the effectiveness of image rotation for open set domain adaptation. In *European Conference on Computer Vision*, pages 422–438. Springer, 2020. 2, 4, 9, 10, 14
2. Zhangjie Cao, Mingsheng Long, Jianmin Wang, and Michael I Jordan. Partial transfer learning with selective adversarial networks. In *Proceedings of the IEEE conference on computer vision and pattern recognition*, pages 2724–2732, 2018. 3
3. Zhangjie Cao, Lijia Ma, Mingsheng Long, and Jianmin Wang. Partial adversarial domain adaptation. In *Proceedings of the European Conference on Computer Vision (ECCV)*, pages 135–150, 2018. 1, 3
4. Zhangjie Cao, Kaichao You, Mingsheng Long, Jianmin Wang, and Qiang Yang. Learning to transfer examples for partial domain adaptation. In *Proceedings of the IEEE/CVF Conference on Computer Vision and Pattern Recognition*, pages 2985–2994, 2019. 1, 3
5. Jia Deng, Wei Dong, Richard Socher, Li-Jia Li, Kai Li, and Li Fei-Fei. Imagenet: A large-scale hierarchical image database. In *2009 IEEE conference on computer vision and pattern recognition*, pages 248–255. Ieee, 2009. 10
6. Qianyu Feng, Guoliang Kang, Hehe Fan, and Yi Yang. Attract or distract: Exploit the margin of open set. In *Proceedings of the IEEE/CVF International Conference on Computer Vision*, pages 7990–7999, 2019. 4
7. Bo Fu, Zhangjie Cao, Mingsheng Long, and Jianmin Wang. Learning to detect open classes for universal domain adaptation. In *European Conference on Computer Vision*, pages 567–583. Springer, 2020. 2, 4, 9, 10, 11
8. Yaroslav Ganin and Victor Lempitsky. Unsupervised domain adaptation by back-propagation. In *International conference on machine learning*, pages 1180–1189. PMLR, 2015. 1
9. Boqing Gong, Kristen Grauman, and Fei Sha. Connecting the dots with landmarks: Discriminatively learning domain-invariant features for unsupervised domain adaptation. In *International Conference on Machine Learning*, pages 222–230. PMLR, 2013. 1
10. Kaiming He, Xiangyu Zhang, Shaoqing Ren, and Jian Sun. Deep residual learning for image recognition. In *Proceedings of the IEEE conference on computer vision and pattern recognition*, pages 770–778, 2016. 10
11. Jogendra Nath Kundu, Naveen Venkat, R Venkatesh Babu, et al. Universal source-free domain adaptation. In *Proceedings of the IEEE/CVF Conference on Computer Vision and Pattern Recognition*, pages 4544–4553, 2020. 10
12. Guangrui Li, Guoliang Kang, Yi Zhu, Yunchao Wei, and Yi Yang. Domain consensus clustering for universal domain adaptation. In *IEEE/CVF Conference on Computer Vision and Pattern Recognition (CVPR)*, 2021. 2, 4, 9, 10, 11
13. Jian Liang, Yunbo Wang, Dapeng Hu, Ran He, and Jiashi Feng. A balanced and uncertainty-aware approach for partial domain adaptation. In *Computer Vision—ECCV 2020: 16th European Conference, Glasgow, UK, August 23–28, 2020, Proceedings, Part XI 16*, pages 123–140. Springer, 2020. 1, 3

14. Hong Liu, Zhangjie Cao, Mingsheng Long, Jianmin Wang, and Qiang Yang. Separate to adapt: Open set domain adaptation via progressive separation. In *Proceedings of the IEEE/CVF Conference on Computer Vision and Pattern Recognition*, pages 2927–2936, 2019. 1, 4
15. Mingsheng Long, Han Zhu, Jianmin Wang, and Michael I Jordan. Unsupervised domain adaptation with residual transfer networks. *arXiv preprint arXiv:1602.04433*, 2016. 1
16. Pau Panareda Busto and Juergen Gall. Open set domain adaptation. In *Proceedings of the IEEE International Conference on Computer Vision*, pages 754–763, 2017. 1, 3
17. Adam Paszke, Sam Gross, Francisco Massa, Adam Lerer, James Bradbury, Gregory Chanan, Trevor Killeen, Zeming Lin, Natalia Gimelshein, Luca Antiga, et al. Pytorch: An imperative style, high-performance deep learning library. *Advances in neural information processing systems*, 32:8026–8037, 2019. 9
18. Xingchao Peng, Qinxun Bai, Xide Xia, Zijun Huang, Kate Saenko, and Bo Wang. Moment matching for multi-source domain adaptation. In *Proceedings of the IEEE/CVF International Conference on Computer Vision*, pages 1406–1415, 2019. 9
19. Xingchao Peng, Ben Usman, Neela Kaushik, Judy Hoffman, Dequan Wang, and Kate Saenko. Visda: The visual domain adaptation challenge. *arXiv preprint arXiv:1710.06924*, 2017. 9
20. Kate Saenko, Brian Kulis, Mario Fritz, and Trevor Darrell. Adapting visual category models to new domains. In *European conference on computer vision*, pages 213–226. Springer, 2010. 9
21. Kuniaki Saito, Donghyun Kim, Stan Sclaroff, and Kate Saenko. Universal domain adaptation through self supervision. *arXiv preprint arXiv:2002.07953*, 2020. 9, 10, 11
22. Kuniaki Saito and Kate Saenko. Ovanet: One-vs-all network for universal domain adaptation. *arXiv preprint arXiv:2104.03344*, 2021. 2, 3, 4, 9, 10, 11, 12, 14
23. Kuniaki Saito, Kohei Watanabe, Yoshitaka Ushiku, and Tatsuya Harada. Maximum classifier discrepancy for unsupervised domain adaptation. In *Proceedings of the IEEE conference on computer vision and pattern recognition*, pages 3723–3732, 2018. 1
24. Kuniaki Saito, Shohei Yamamoto, Yoshitaka Ushiku, and Tatsuya Harada. Open set domain adaptation by backpropagation. In *Proceedings of the European Conference on Computer Vision (ECCV)*, pages 153–168, 2018. 1, 4, 10, 14
25. Karen Simonyan and Andrew Zisserman. Very deep convolutional networks for large-scale image recognition. *arXiv preprint arXiv:1409.1556*, 2014. 13, 14
26. Hemanth Venkateswara, Jose Eusebio, Shayok Chakraborty, and Sethuraman Panchanathan. Deep hashing network for unsupervised domain adaptation. In *Proceedings of the IEEE conference on computer vision and pattern recognition*, pages 5018–5027, 2017. 9
27. Kaichao You, Mingsheng Long, Zhangjie Cao, Jianmin Wang, and Michael I Jordan. Universal domain adaptation. In *Proceedings of the IEEE/CVF conference on computer vision and pattern recognition*, pages 2720–2729, 2019. 2, 4, 10, 11
28. Jing Zhang, Zewei Ding, Wanqing Li, and Philip Ogunbona. Importance weighted adversarial nets for partial domain adaptation. In *Proceedings of the IEEE conference on computer vision and pattern recognition*, pages 8156–8164, 2018. 1, 3
29. Yang Zou, Zhiding Yu, BVK Kumar, and Jinsong Wang. Unsupervised domain adaptation for semantic segmentation via class-balanced self-training. In *Proceed-*

ings of the European conference on computer vision (ECCV), pages 289–305, 2018.

1